The geology of Damavand volcano, Alborz Mountains, northern Iran

Jon Davidson†
Department of Earth and Space Sciences, University of California, Los Angeles, California 90095-1567, USA, and *Department of Earth Sciences, University of Durham, Durham, DH1 3LE, UK*

Jamshid Hassanzadeh
Department of Geology, Faculty of Science, and Institute of Geophysics, Tehran University, P.O. Box 14155-6466, Tehran, Iran

Reinis Berzins
Department of Earth and Space Sciences, University of California, Los Angeles, California 90095-1567, USA, and *GSi/water, 520 Mission Street, South Pasadena, California 91030, USA*

Daniel F. Stockli
Division of Geological and Planetary Sciences, California Institute of Technology, MS 100-25 Pasadena, California 91125, USA, and *Department of Geology, University of Kansas, Lawrence, Kansas 66045, USA*

Behrooz Bashukooh
Department of Geology, Faculty of Science, and Institute of Geophysics, Tehran University, P.O. Box 14155-6466, Tehran, Iran, and *Human and Environment R and D Engineering Company (HEENCO), No. 23, Persia Tower (6th floor, No. 62), Tehran, Iran*

Brent Turrin
Lamont-Doherty Earth Observatory, Columbia University, RT 9W, Palisades, New York 10964, USA, and *Department of Geological Sciences, Rutgers University, Wright Geological Laboratory, 610 Taylor Road, Piscataway, New Jersey 08854-8066, USA*

Ali Pandamouz
Department of Geology, Faculty of Science, and Institute of Geophysics, Tehran University, P.O. Box 14155-6466, Tehran, Iran and *Department of Geology, P.O. Box 4099, Northern Arizona University, Flagstaff, Arizona 86011, USA*

ABSTRACT

Damavand volcano, located in northern Iran, is a large (>400 km^3) composite cone that is currently dormant; it shows fumarolic activity near the summit but no evidence of eruption in the past 1000 yr. The volcano represents an isolated focus of magmatism of uncertain tectonic affinity, although geophysical and geochemical constraints point toward a local hotspot/plume origin, possibly associated with lithospheric delamination, rather than any association with subduction. New (U-Th)/He and ^{40}Ar/^{39}Ar geochronological constraints indicate that the present cone (Young Damavand) has been constructed over ~600 k.y. on an older, eroded edifice of indistinguishable composition (younger than 1.8 Ma). Damavand activity has been characterized by the eruption of radially directed trachyandesite lava flows, almost exclusively from summit vents. Limited pyroclastic activity has yielded thin fallout pumice lapilli layers and a few pyroclastic flows. Only one significant pyroclastic event is recognized in the remnants of a welded ignimbrite, ponded and preserved along the Haraz River drainage.

Relatively short periods of volcanic eruptive activity were interspersed with longer periods of erosion in which volcanic products were transported, particularly as hyperconcentrated flows, into the surrounding drainage systems to be further reworked into epiclastic deposits. Occasional catastrophic events punctuated this interplay between volcanism and erosion. At least one sector collapse is signified by the presence of a large debris avalanche deposit, and the regional drainage systems appear to have been frequently dammed by incursions of volcanic material.

Keywords: Alborz Mountains, Damavand volcano, argon-argon, geochronology, (U-Th)/He, volcanic centers, volcaniclastic rocks.

INTRODUCTION

Damavand volcano is the highest peak in the Middle East; its elevation is 5670 m above sea level. It is a large intraplate composite cone representing an accumulation of more than 400 km^3 of trachyandesite lavas and pyroclastic material overlying the active fold-and-thrust belt of the Alborz Mountains, the range that fringes the southern Caspian Sea (Fig. 1). A preliminary study of the volcano was carried out by Allenbach (1966) that provided a general overview of the geology and nature of the volcanic rocks, and a brief summary of geochemical characters of Damavand volcano was published by Mehdizadeh et al. (2002). This paper presents a summary of our field observations together with an age-calibrated stratigraphic framework of the volcanic and volcaniclastic rocks in order to understand the nature of volcanic activity and the

†E-mail: j.p.davidson@durham.ac.uk.

GSA Bulletin; January/February 2004; v. 116; no. 1/2; p. 16–29; DOI 10.1130/B25344.1; 9 figures; 3 tables.

For permission to copy, contact editing@geosociety.org
© 2004 Geological Society of America

time scales over which activity occurred We also present geochemical data that bear on the origin of magmatism and differentiation processes occurring at the volcano.

REGIONAL GEOLOGY

The Alborz Mountains constitute an active, arcuate fold-and-thrust belt (Stocklin 1974, 1977; Axen et al., 2001). Seismic data suggest that the belt is being compressed and consequently uplifted against the relatively stable block underlying the southern Caspian Sea. This block, in turn, may represent a trapped remnant of Tethyan oceanic lithosphere (Berberian, 1983).

Despite average elevations of >2000 m, the crustal thickness beneath the Alborz Mountains calculated on the basis of gravity data is currently <35 km (Dehghani and Makris, 1984). The central Iranian plateau and the Alborz Mountains may have been overthickened crust following end-Tethyan tectonics (Dilek and Moores, 1999) but are now both largely underlain by anomalously low-density upper mantle (Kadinsky-Cade et al., 1981; Toksoz and Bird, 1977). From seismology, geothermal and volcanic activity, and uplift rates, Hassanzadeh (1994) has inferred that the asthenosphere must be shallower than normal in the central Iranian plateau region.

Jung et al. (1976) suggested that Damavand volcano is related to a recent (as yet unidentified) subduction zone located to the south-southwest and that magmas were generated at ~250 km depth above a north-dipping slab. A modification of this hypothesis (Brousse et al., 1977) related magmatism to a slab that had detached from the Zagros continental block. Priestley et al. (1994) suggested that underthrusting of the Caspian Sea block from the north may represent recent initiation of subduction. However, current subduction beneath Damavand volcano is not supported by seismic data, and no surface expression of an associated trench or suture has been identified. Subduction appears to have ceased here in the late Neogene (e.g., Dewey and Şengör, 1979). Key tectonically discriminant geochemical data such as Nb concentrations and Hf-Th-Ta ratios (presented below) lend little support for a subduction-zone origin. Magmatism is therefore thought to be related to intraplate processes, most likely a local upwelling, leading to decompression melting.

The immediate basement to Damavand volcano in the Alborz Mountains is a folded and thrust-faulted passive-margin sedimentary sequence of carbonate, siliciclastic, and volcanic rocks. The sequence ranges in age from Cambrian to Eocene. Jurassic passive-margin deposits are represented by the clastic (sandstone-shale) Shemshak Formation, and the Lar and Delichi carbonates. The Eocene Karadj Formation comprises tuffs, largely submarine (and altered to exhibit a distinctive green color) and suggestive of the onset of active continental-margin magmatism. The structural fabric of faults and fold axes is oriented largely east-west, parallel to the Alborz Mountains (Fig. 1).

A series of small olivine basalt flows in the Damavand region (Fig. 1) signifies at least limited magmatism prior to the most recent volcanism localized at Damavand volcano. These basalts are petrographically and geochemically distinct from the Damavand trachyandesites (Pandamouz, 1998; Davidson et al., 2000).

FIELD GEOLOGY, PETROLOGY, AND STRATIGRAPHY OF DAMAVAND VOLCANO

General Morphology of the Edifice

The current cone of Damavand volcano (Fig. 1), informally termed ''Young Damavand'' rests upon an eroded apron of earlier deposits related to the eruption of ''Old Damavand.'' There is no distinction in either the mineral assemblages or compositions of rocks from the two phases, and a broadly continuous history of magmatism at this location over the past 1 m.y. or longer is envisaged. However, an unconformity between the two series of lavas is observed in Gazaneh Canyon on the northeast flanks (Fig. 2A). The attitude of the lower lavas, which dip toward the current cone, is suggestive of an earlier center located slightly to the north and east of the current cone. This interpretation is also consistent with the morphology of the volcanic deposits in the northern part of the area (Fig. 2B). Sardobitch, an arcuate ridge of lavas (dipping gently northward), was interpreted by Allenbach (1966) as a caldera wall. However, no pyroclastic deposits have been found that might correlate with a caldera-forming event of this age and magnitude. This ridge is more likely to be the deeply eroded remnant flanks of Old Damavand, and the southern flanks are buried beneath the current cone, represented by the lower lavas in Figure 2A. Erosion may have been accelerated by the vulnerability of hydrothermally altered rocks in the interior of Old Damavand, vestiges of which are seen high on the ridge above Gazaneh Canyon, as well as the relatively high elevation of the edifice. A thick sequence of volcaniclastic rocks, comprising mainly alluvium and lahars, occupies the Hadjidella valley to the north of the current cone (Figs. 1, 2B). Excavation of the interior of the old cone transported material eastward into the Haraz drainage; the Haraz River then carried the sediment northward to the Caspian Sea.

The geomorphology of the Young Damavand edifice may similarly support the suggestion that there has been a slight but significant shift in the locus of the main eruptive vent; flows become apparently progressively younger toward the south and west. Only one significant satellite vent has been identified, a young dome-flow complex on the southern flank (Fig. 1A), although there may be additional small dome complexes such as one found high on the northeast flanks near the climbers' shelter. The flows on the eastern flanks are morphologically subdued and include significant inliers of sedimentary basement at relatively high elevation. In the northeastern sector of the cone in particular, few distinct individual flows can be identified.

The uppermost part of the young cone is steep, and small-volume trachyandesite flows are radially disposed about the present summit region (Fig. 1). The summit crater is filled with nieve penitents—ice pinnacles thought to be formed by sublimation and redeposition due to solar radiation in an arid climate. Two small glaciers, which have retreated even since 1930, are recognized in the summit region and are the remnants of more extensive glaciers that existed in the Pleistocene (Ferrigno, 1991). The steepest flanks of the volcano are along the western side and are formed almost exclusively of young lava flows. Morphologically, these flows exhibit distinct flow levees and commonly blocky top surfaces that have not been affected by glaciation.

Pyroclastic rocks are subordinate to lavas. With the exception of a significant ignimbrite deposit found along the Haraz Valley, pyroclastic deposits are mainly fallout deposits and are found on—or near—the present surface of the edifice. The deposits have typically been reworked into swales and depressions, which has given rise to common clast rounding and fluvial sedimentary structures such as cross-bedding and channeling. In quarries where the incipiently reworked pumice deposits are several meters thick, large black and gray and banded pumice clasts are found. The bands have the same composition; the striking color difference is merely a function of degree of vesicularity between a gray, highly vesicular pumice and a dark, less vesicular pumice. On the southwest flanks, a series of thin pyroclastic flows and falls are exposed. None of these is welded, although some consolidation of the flows may be due to vapor-phase alteration. The deposits are invariably incipiently reworked.

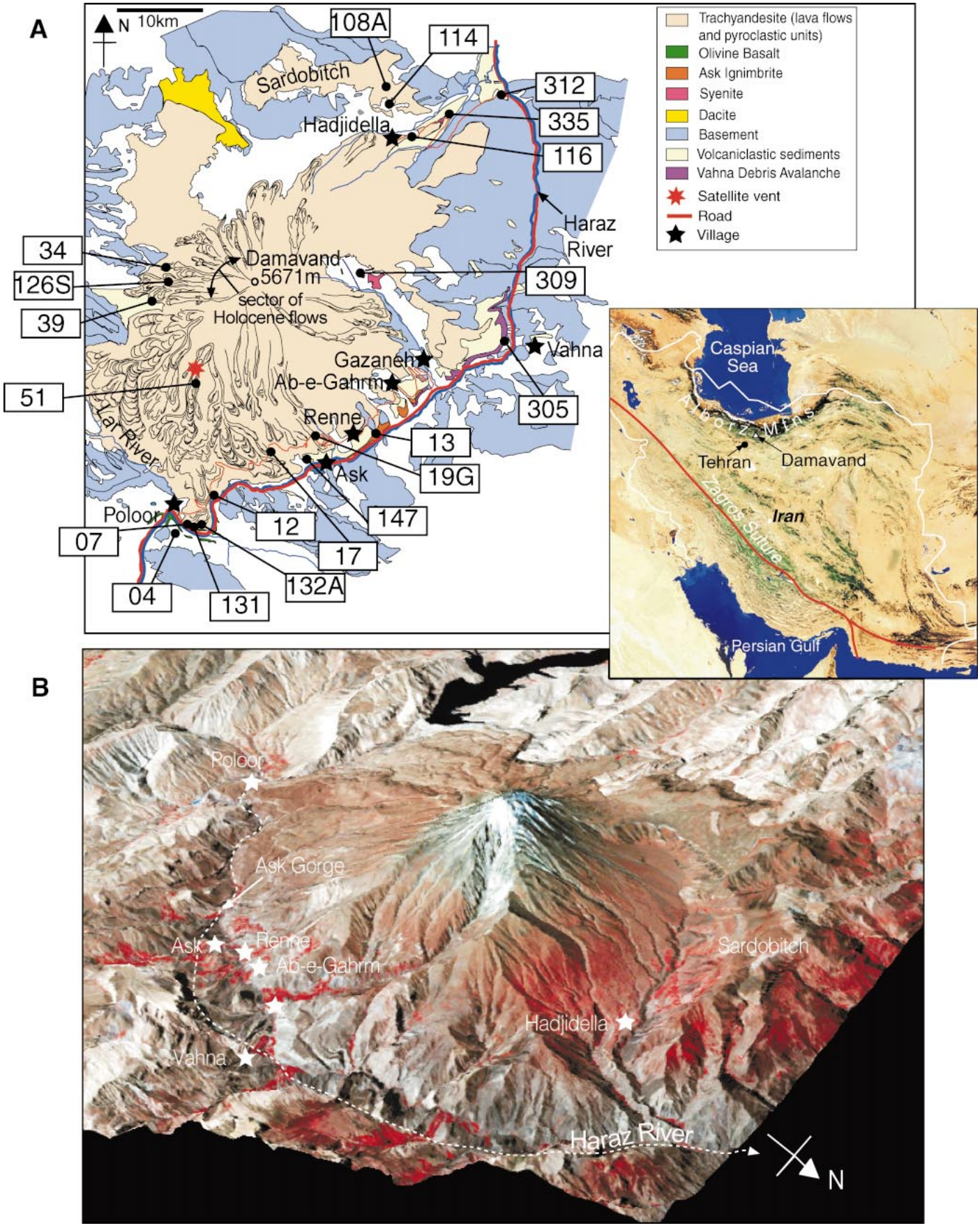
A
N 10km
Trachyandesite (lava flows and pyroclastic units)
Olivine Basalt
Ask Ignimbrite
Syenite
Dacite
Basement
Volcaniclastic sediments
Vahna Debris Avalanche
Satellite vent
Road
Village
108A
114
312
335
116
Sardobitch
Hadjidella
Haraz River
34
126S
39
Damavand 5671m
sector of Holocene flows
309
Vahna
Gazaneh
Ab-e-Gahrm
305
51
Lar River
Renne
13
19G
Ask
Poloor
12
147
07
17
132A
04
131
Caspian Sea
Alborz Mts
Tehran
Damavand
Iran
Zagros Suture
Persian Gulf
B
Poloor
Ask Gorge
Ask
Renne
Ab-e-Gahrm
Sardobitch
Hadjidella
Vahna
Haraz River
N

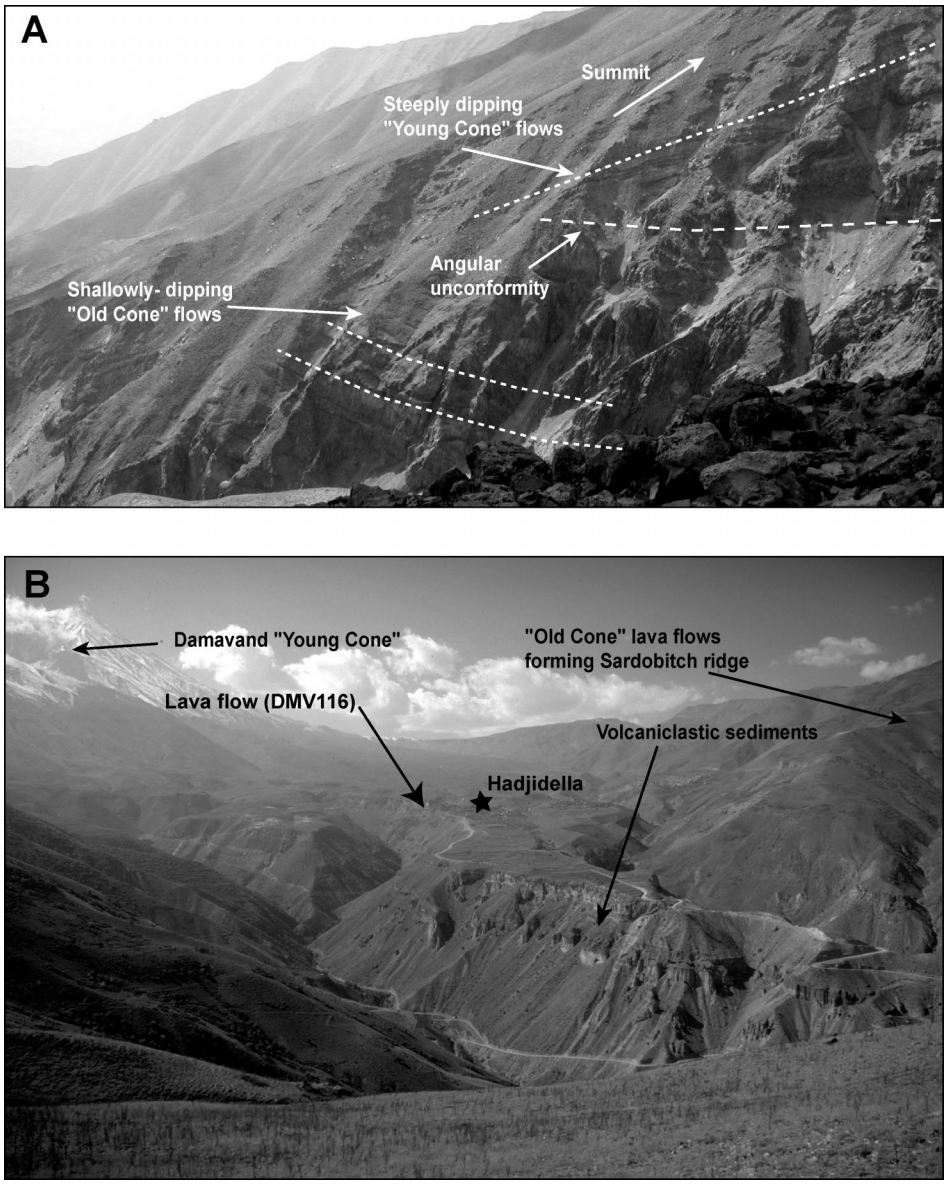

Figure 2. Relationship between the older and younger volcanic deposits. (A) Unconformity between Old Damavand deposits and Young Damavand lavas exposed in Gazaneh Canyon. Width of image represents ~200 m. (B) Northeast flanks of the cone; view to the west. Sardobitch ridge to the north (right) comprises older lavas—the remains of Old Damavand volcano—and the broad intervening valley is filled with volcaniclastic sediments of the Hadjidella formation that were transported eastward to the main Haraz River drainage. The sediments are capped in the middle distance by flows from Young Damavand. The valley is ~5 km across.

Petrography and Geochemistry

Over 100 samples have been analyzed for major and trace element contents (many additionally for isotope ratios). All are trachyandesites, varying in SiO_2 content only between 57% and 64% (Table 1 and Fig. 3). There are no significant differences in composition between rocks from Old and Young Damavand. The compositions of all pyroclastic rocks sampled are indistinguishable from those of the associated lavas (with the exception of a small inter-lava tephra layer—DMV117—in the canyon below Hadjidella, which may be from an unidentified external source; Fig. 3A). Furthermore, there are no significant differences in mineral assemblages among the rocks. A disequilibrium assemblage of ternary feldspar + clinopyroxene + apatite + oxide ± biotite ± amphibole is found in all samples. Apatites are large—up to 5 mm—and typically euhedral. Feldspars are commonly resorbed and riddled with melt inclusions, whereas hydrous minerals are rimmed by or replaced with opacite.

Geochemical data from Damavand trachyandesites indicate an association with intraplate magmatic suites. On a Ti/Y vs. Nb/Y discriminant diagram (Fig. 4A), Damavand trachyandesites fall close to the within-plate basalt field and do not overlap with the field for volcanic arc rocks, whereas in the Hf-Th-Ta triangular discriminant diagram (Fig. 4B), the trachyandesites fall between the two fields. Tectonic-environment discriminant diagrams are strictly only valid for primitive rocks, and the Damavand rocks are highly differentiated. Low Y contents and high Th contents are likely due to crustal contamination and concomitant fractionation of amphibole and apatite—such differentiation processes cause the Damavand rocks to plot in rather equivocal areas of the discriminant diagrams. Fractionation of observed phases such as magnetite and apatite can create considerable scatter in trace element characteristics. Fractionation vectors (Fig. 4A) suggest that parental magmas probably had lower Nb/Y ratios, while providing little constraint on parental Ti/Y ratios. Basalts from the region, which might represent parental magmas, do have lower Nb/Y ratios and plot closer to the ''within-plate'' fields (Figs. 4A and 4B).

Damavand trachyandesites have much high-

Figure 1. (A) Sketch map (after Cartier, 1972) of Damavand. Locations of dated samples from Table 2 and 3 are shown and labeled (sample numbers abbreviated without prefix DMV). Inset shows setting of Damavand volcano in regional context in northern Iran, just south of the Caspian Sea and northeast of Tehran. (B) Digital elevation model (DEM) of Damavand volcano (data courtesy of the Iranian Remote Sensing Center). Main localities labeled are those mentioned in the text.

TABLE 1. REPRESENTATIVE GEOCHEMICAL ANALYSES OF DAMAVAND ROCKS

	Young Damavand									Old Damavand			Regional basalts
	DMV12	DMV13	DMV19G	DMV19B	DMV34	DMV147	DMV07	DMV116	DMV39	DMV132A	DMV114	DMV108	DMV10
Age (ka)	25	280	180	180	7	450	27	200	180	810	1030	970	>800
SiO_2	60.68	62.60	59.18	59.30	60.63	61.20	60.24	62.04	59.39	61.32	62.31	60.13	48.92
TiO_2	1.09	0.90	1.05	1.09	1.07	1.04	1.03	0.94	1.11	1.01	0.99	1.10	1.81
Al_2O_3	15.78	15.56	15.28	15.32	15.90	16.01	15.62	15.58	15.41	15.87	15.79	15.72	14.47
Fe_2O_3	5.11	3.02	4.98	5.07	5.17	5.09	4.88	4.68	5.14	4.87	4.81	5.27	8.67
MnO	0.07	0.05	0.08	0.07	0.07	0.07	0.07	0.06	0.07	0.06	0.06	0.08	0.12
MgO	2.72	2.15	2.59	2.73	2.76	2.22	2.53	2.69	2.75	2.61	2.37	3.02	8.06
CaO	4.90	3.55	4.40	4.47	4.36	4.08	4.70	4.23	4.49	4.08	3.80	4.44	8.83
P_2O_5	0.67	0.53	0.67	0.66	0.62	0.59	0.62	0.52	0.69	0.59	0.55	0.61	1.28
Na_2O	4.75	4.56	4.84	4.74	4.78	4.87	4.82	4.73	4.80	4.79	4.69	4.71	4.40
K_2O	4.42	4.61	4.41	4.37	4.36	4.32	4.39	4.43	4.43	4.39	4.31	4.26	1.77
LOI	0.05	2.46	1.51	2.03	0.52	0.51	0.82	0.01	1.45	0.23	0.14	0.66	1.68
Total	100.23	99.99	98.98	99.85	100.23	99.98	99.70	99.90	99.73	99.82	99.82	99.99	100.01
V	*77*	*61*	75	*77*	*72*	62	*75*	58	*76*	58	60	66	*155*
Cr	*54*	*55*	40	*61*	*65*	42	*54*	70	*51*	62	42	70	*294*
Ni	*39*	*28*	30	*46*	*45*	22	*37*	40	*44*	38	24	44	*232*
Ga	*20*	*16*	22	*23*	*15*	23	*11*	23	*21*	24	23	23	*14*
Rb	*125*	*163*	135	*125*	*117*	128	*126*	141	*121*	130	126	117	*75*
Sr	*1704*	*1209*	1492	*1632*	*1406*	1220	*1621*	1300	*1430*	1340	1210	1340	*3209*
Y	*13*	*13*	11	*12*	*13*	14	*12*	13	*11*	14	15	14	*29*
Zr	*306*	*314*	385	*350*	*293*	378	*329*	373	*334*	356	325	352	*376*
Nb	*56*	*56*	61	*62*	*56*	58	*57*	58	*59*	56	50	54	*60*
Ba	*1240*	*1202*	1345	*1234*	*1229*	1281	*1314*	1335	*1230*	1286	1247	1252	*2227*
La	*95.2*	*96.1*	79	*100.4*	*89.4*	80	*95.5*	86	*92.3*	84	68	86	*144.1*
Ce	*174.3*	*170.0*	171	*173.9*	*160.1*	152	*173.1*	175	*159.8*	160	152	150	*249.6*
Nd	*56.4*	*53.9*	60	*58.1*	*55.7*	40	*54.6*	45	*55.2*	45	35	45	*97.9*
Sm	*8.0*	*7.4*	–	*7.9*	*8.0*	–	*7.6*	–	*7.4*	–	–	–	*13.4*
Eu	*2.0*	*1.8*	–	*2.1*	*2.1*	–	*1.9*	–	*2.0*	–	–	–	*3.4*
Gd	*5.8*	*5.6*	–	*5.6*	*6.0*	–	*5.4*	–	*5.4*	–	–	–	*9.0*
Yb	*1.1*	*1.1*	–	*1.0*	*1.3*	–	*1.1*	–	*1.0*	–	–	–	*1.7*
Hf	*7.5*	*7.1*	13	*7.8*	*7.9*	10	*7.2*	10	*7.6*	11	9	11	*6.4*
Ta	*3.7*	*3.8*	7	*4.2*	*4.2*	6	*3.9*	9	*3.9*	5	7	8	*2.9*

Note: Major and trace element analyses by XRF (X-ray fluorescence; courtesy of R. Arculus, Australian National University), trace element data in italics by ICP-MS (inductively coupled plasma–mass spectrometry; courtesy of C. Neal, University of Notre Dame). Sample locations in Fig. 1, approximate ages—details in Table 2.

er Nb contents ($\gg$40 ppm) than might be expected of subduction-related magmas, which clearly distinguishes them from similarly differentiated continental volcanic arc rocks (Fig. 4C). The Damavand trace element signature is broadly similar to that of intraplate trachytes from Sudan (Jebel Marra); differences in Sr and HREEs (heavy rare earth elements) reflect the relative importance of fractionating feldspar and amphibole, respectively (Fig. 4C). The absence of trace element indicators of a subduction origin seems to confirm general tectonic and geophysical evidence presented above that active subduction has not affected the Alborz Mountains since at least 1 Ma.

The apparent geochemical intraplate affinity is not obviously associated with a significant plume. Other than Damavand volcano, there is very limited magmatism in the region, and no reported regional doming. An alternative is that Damavand volcano represents a local hotspot formed by decompression melting of rising asthenosphere in response to complementary lithospheric delamination (e.g., Pearce et al., 1990). The occurrence of delamination is consistent with the ''normal'' crustal thicknesses (~30 km; Dehghani and Makris, 1984) associated with the elevated Alborz Mountains, which suggests that the crust is supported dynamically. However, the geochemistry, especially the isotopic compositions (Young et al., 1998), cannot be produced by simple asthenospheric melting without additional contributions from an incompatible element–enriched reservoir, most likely the lithosphere.

At Damavand volcano there are no distinctive compositions or apparent trends through time in major trace or isotopic compositions that can be used for correlative purposes. Thus chemical stratigraphic methods that have been used successfully elsewhere (e.g., Singer et al., 1997; Wörner et al., 1988) have not proved useful.

Stratigraphy Along the Haraz River Drainage

The Haraz River drainage, located along the eastern side of Damavand volcano (Fig. 1), plays a fundamental role in modulating the topography of the volcano. The drainage is one of a few major south-to-north–flowing systems that cross the Alborz Mountains and flow into the Caspian Sea. In the southern part of the area toward Poloor, deposits in the lower part of the volcanic succession attest to episodes of damming of the drainage due to lava flows from the volcano or as a consequence of landslides from the steep valley walls. The current drainage system reflects such activity; between field seasons in 1997 and 1998, collapse of a perched travertine terrace southeast of Ask led to the development of a small dam and lake along the river, and a cascade over the collapse debris is currently reincising the river's channel. Similarly, aggradation in a small basin has been caused by damming of the Lassem River tributary southwest of the volcano, in which minor stream braiding has developed.

In the Haraz drainage, paleo–river terraces define episodes of fluvial sedimentation alternating with mass flows (lava flows, debris flows, etc.) from the topographically high volcano to the west. These volcaniclastic deposits are exposed almost entirely only in canyon walls on the west side of the river or in the valleys of tributaries along the western flanks of the volcano, suggesting that the drainage has shifted eastward through time to accommodate the expanding footprint of the volcano through a complex interplay of volcanic deposition and erosional processes. Summary stratigraphic logs are provided in Figure 5, following detailed work by Berzins (2001). The arcuate trace of the drainage around the

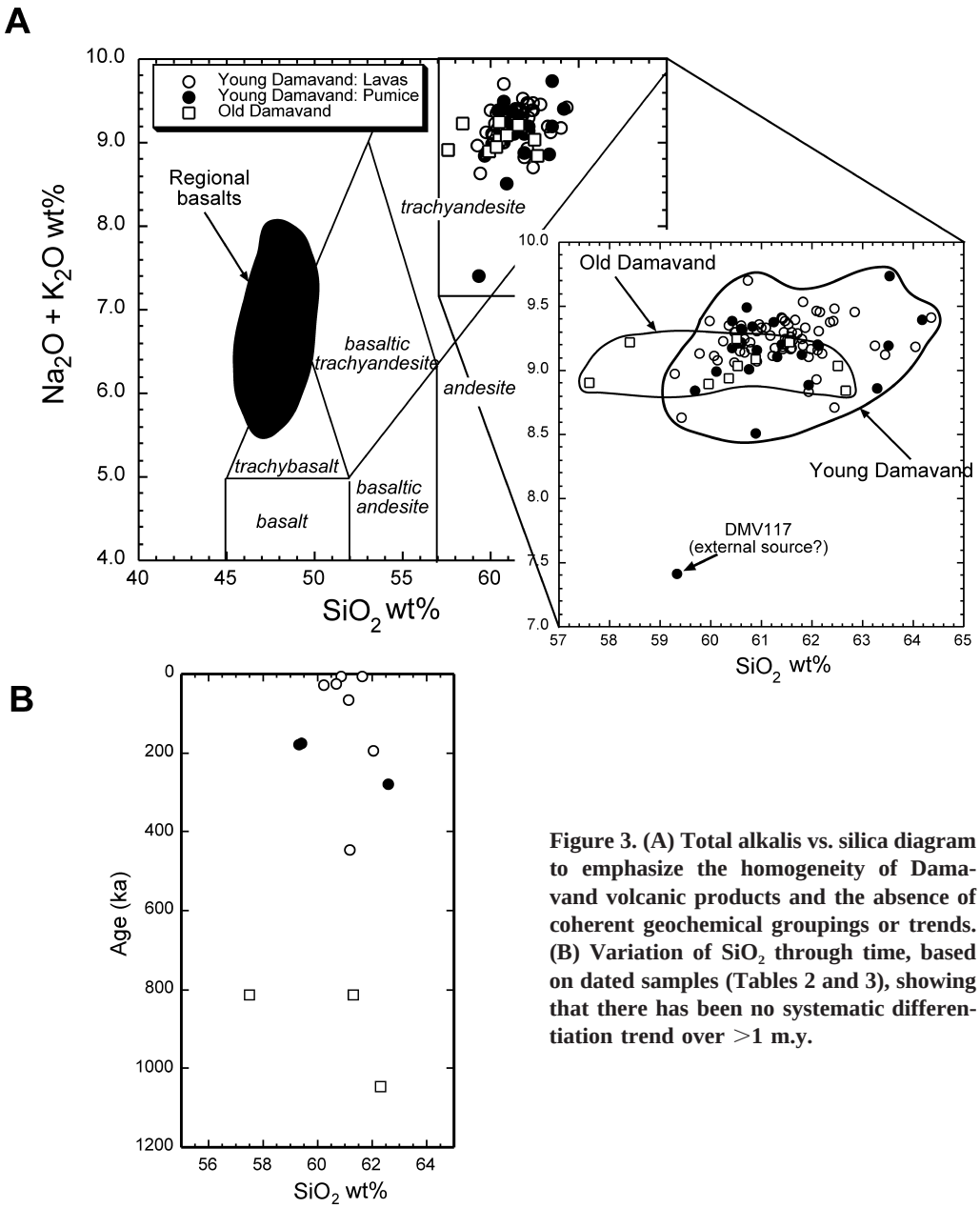

Figure 3. (A) Total alkalis vs. silica diagram to emphasize the homogeneity of Damavand volcanic products and the absence of coherent geochemical groupings or trends. (B) Variation of SiO_2 through time, based on dated samples (Tables 2 and 3), showing that there has been no systematic differentiation trend over >1 m.y.

volcano, convex toward the east, may support the interpretation of an eastward-shifting drainage (Fig. 1).

The effect of mass flows on the drainage is exemplified by the stratigraphic relationships around Ask Gorge (Figs. 5, 6A). The Ask Gorge is formed where the Haraz River has cut a gorge through a ridge of resistant Lar Limestone. The current valley has been displaced from an earlier course farther to the west by a thick, canyon-filling trachyandesite (the ''lava flow'' of Fig. 6A). The Ask Gorge separates distinct volcaniclastic facies along the Haraz drainage; older units lie to the south. Pronounced erosion of volcaniclastic deposits and lateral channel migration has taken place in many additional places along the Haraz River drainage (Fig. 6B).

Stratigraphy South of the Ask Gorge

To the south of the Ask Gorge are found the oldest sedimentary deposits, largely fluvial sediments, which are intercalated with olivine basalt flows near the village of Poloor. The sediments, informally referred to as the ''Poloor formation,'' are uniformly light cream colored to green, relatively fine grained, and well bedded. The green color is largely a reflection of incorporation of eroded debris from green tuffs of the Eocene Karadj Formation. Much of the sediment comprises fine-grained, reworked pumice and ash, compositionally similar to the main Damavand cone. When compared with the sediments exposed immediately to the north of Ask Gorge, the sediments of the Poloor formation contain a far higher proportion of basement material and are more strongly fluvially reworked.

The olivine basalts are small in volume and local in distribution; they fill channels and valleys cut into the Poloor formation deposits (Pandamouz, 1998). They therefore now occur as remnants inset against valley walls along the main drainage, stratigraphically overlying at least some of these sediments. They were likely erupted from local cinder cones, although the locations of these sources are now

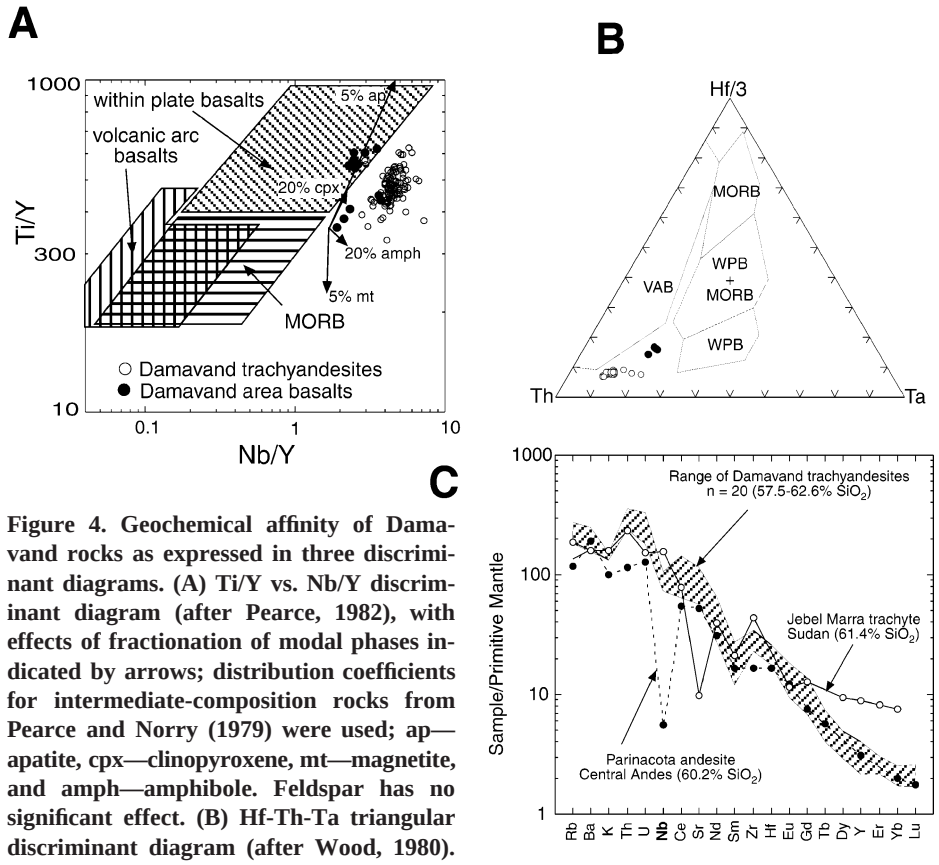

Figure 4. Geochemical affinity of Damavand rocks as expressed in three discriminant diagrams. (A) Ti/Y vs. Nb/Y discriminant diagram (after Pearce, 1982), with effects of fractionation of modal phases indicated by arrows; distribution coefficients for intermediate-composition rocks from Pearce and Norry (1979) were used; ap—apatite, cpx—clinopyroxene, mt—magnetite, and amph—amphibole. Feldspar has no significant effect. (B) Hf-Th-Ta triangular discriminant diagram (after Wood, 1980). (C) Primitive mantle–normalized diagram of incompatible trace element abundances (normalization constants from Sun and McDonough, 1989). Andean andesite (PAR82) and Jebel Marra trachyte (X81), both within the SiO_2 range of the Damavand trachyandesites, are from Davidson et al. (1990) and Davidson and Wilson (1989), respectively.

obscure. Additional small outcrops of olivine basalt occur in the general area to the east of the map area of Figure 1A, and it is likely that these are related to those in the Poloor area. Damavand lavas overlie the basalts, although trachyandesite and pumice clasts, with typical Damavand chemical compositions, in the sediments indicate that the earliest trachyandesite activity was penecontemporaneous with the olivine basalts.

Stratigraphy North of the Ask Gorge

The key stratigraphic sections at Ask, Abe-Gahrm, Gazaneh, and Hadjidella (Fig. 5) are all distinctly different from the Poloor formation; they comprise principally coarse-grained fluvial to hyperconcentrated flow deposits. We have informally divided these volcaniclastic successions into the older ''Hadjidella formation,'' represented in all four key sections, and the younger ''Ask formation,'' represented only in the three southern key sections. The general variation within the succession is from deposits dominated by hyperconcentrated or debris flows into those dominated by fluvial deposits. This variation is observed both up section at Hadjidella and laterally from Hadjidella southward to Ask.

The abundance of Mesozoic basement clasts, although never large, decreases up section. Hydrothermally altered volcanic clasts similarly decrease in abundance up-section. Pumice-rich horizons are rare, discontinuous, and reworked, so they do not form good chronostratigraphic horizons. Intercalated roughly between the two formations are at least two marker horizons (Fig. 5), an ignimbrite (the Ask Ignimbrite) and a debris avalanche deposit (the Vahna debris avalanche).

The Vahna debris avalanche is best exposed along the Haraz River valley near Vahna (Fig. 1), where it forms a cliff ~60 m in height directly overlying basement rocks. The deposit itself, where well preserved, comprises a classic jigsaw breccia of trachyandesite. However, the deposit is only exposed in sections intercalated between volcaniclastic deposits, so no hummocky top surface (as would typically be used to identify debris avalanche deposits) is seen. The Vahna debris avalanche can be traced south along the Haraz River valley until it ends at the north side of Ab-e-Gahrm Valley. Stratigraphically above the Vahna debris avalanche are a series of fluvial sediments that are, in turn, overlain by the Ask Ignimbrite, which is dated at ca. 280 ka (Tables 2 and 3).

The Ask Ignimbrite (Fig. 5) is moderately welded and columnar-jointed toward its base in its thickest parts (up to 100 m just north of Ask) and may have erupted from the location of the current cone—although it is currently found only in the Haraz drainage. The fact that we have found no caldera-like structures that might represent a source for the deposit suggests that its vent (or vents) is (are) buried beneath deposits of Young Damavand, which have accumulated a significant edifice in the past 280 k.y. The lithic content of the ignimbrite is variable and includes altered trachyandesite and basement rocks. Extrapolation of typical thicknesses over the area of the Haraz River valley occupied by the Ask Ignimbrite gives a minimum original volume of a few cubic kilometers, although estimates are poor owing to ponding and subsequent extensive erosion. Intense welding in places probably results from the rather alkaline composition of the magma compared with calc-alkaline rhyolitic magmas (e.g., Schmincke, 1974; Wolff and Wright, 1981).

GEOCHRONOLOGY

There are no historical records of eruption of Damavand volcano. At present there are active fumaroles and sulfur encrustations in the summit region that attest to an extant heat source. The scarcity of distinct, laterally extensive chronostratigraphic marker horizons and the petrographic and chemical similarity of the lavas (Fig. 3) have impeded attempts to establish a calibrated rock succession.

The eruptive history of the Damavand volcanic edifice can be quantified, however, by using radioisotope dating methods. Carbon dates of ca. 38 ka are reported from lake terraces formed as a consequence of the natural damming of the Lar River by lavas from the southwestern flank of the volcano (Allenbach, 1966). However, searches for datable charcoal samples beneath the more recent flows were unsuccessful, probably a consequence of the lack of substantial vegetation in the arid climate of the central Alborz Mountains. We therefore employed Ar/Ar and (U-Th)/He isotope dating methods to determine the ages of key eruptions.

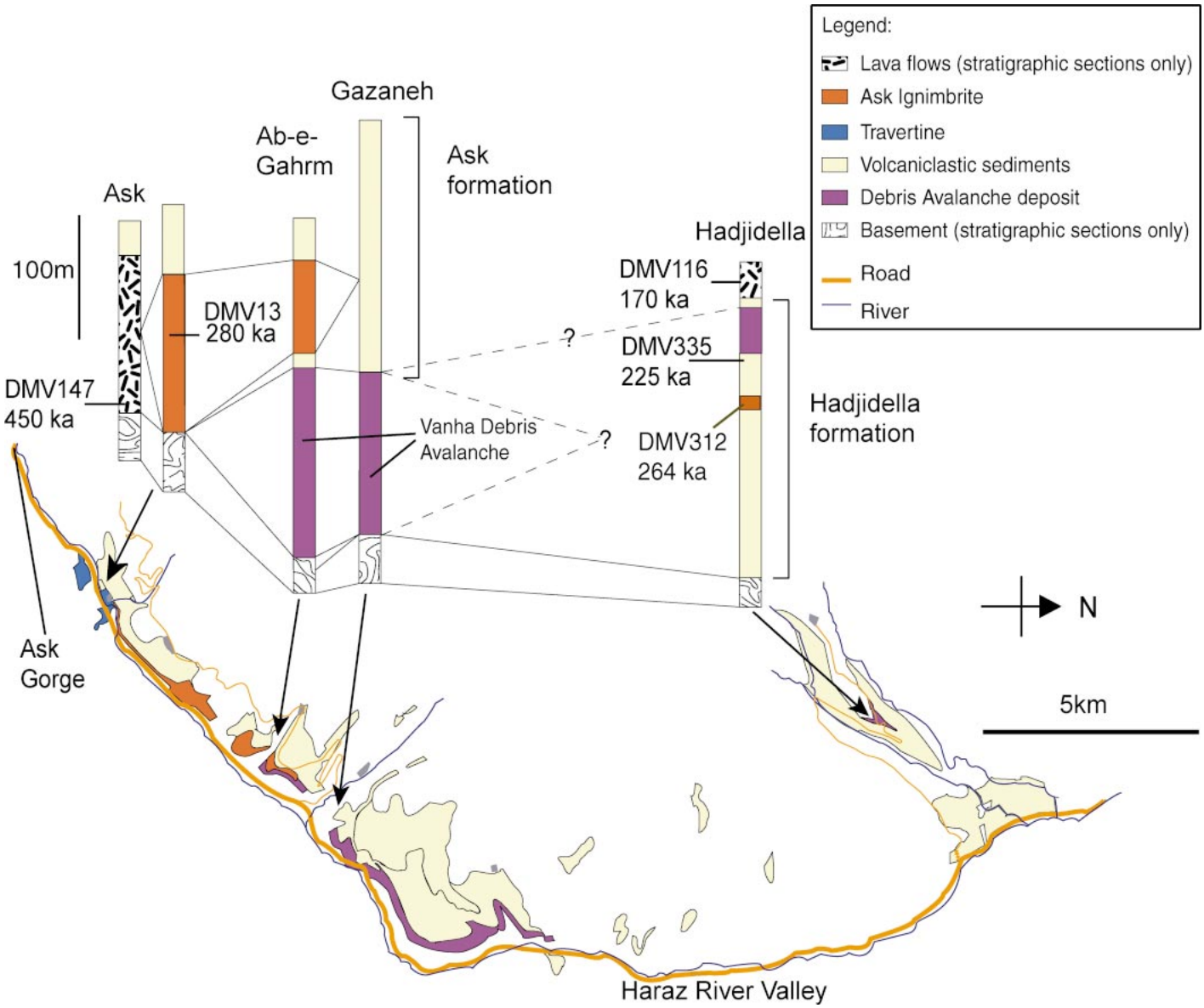

Figure 5. Schematic stratigraphic logs of key sections along the Haraz River drainage and its tributaries with locations projected to the geologic map (see Fig. 1 for locations in context). Correlations and radioisotope age calibrations are indicated. "Basement" comprises limestone, sandstone, and shale of the Lar, Delichi, and Shemshak Formations.

^{40}Ar-^{39}Ar Dating

Despite the potassic nature of the Damavand volcanic rocks, reliable Ar isotope ages have proven very difficult to obtain, probably because of the disequilibrium state of many of the minerals. Initial experiments with biotite crystals were plagued by excess nonatmospheric ^{40}Ar, giving ages in the 0.5 Ma range, but with errors of 20%–50%. Subsequent ^{40}Ar/^{39}Ar geochronology performed at Lamont Doherty yielded data presented in Table 2 and Figure 7. Sample locations are shown in Figure 1. Techniques are described in Turrin et al. (1998) and Figure 8. The difficulties in obtaining argon isotope ages are illustrated by reference to the details of argon isotope analyses presented in Table 2. From this it is clear that, for many samples, the isochron and plateau ages obtained from the same sample are not in agreement. On some samples where biotite was analyzed in addition to feldspar (DMV51 and DMV13), the two minerals give different ages. Samples such as DMV108—for which plateau and isochron ages are identical, the isochron MSWD (mean square of weighted deviates) is low, and the initial argon isotope composition is atmospheric—are the exception. Consequently, each analysis needed individual scrutiny in order to pick the "best" age, by using criteria such as plateau shape, release spectrum, and isochron MSWD. These "preferred ages" are indicated in boldface in Table 2.

The criteria used to determine the most reliable ^{40}Ar/^{39}Ar age deserve some explanation. Twelve samples were selected for ^{40}Ar/^{39}Ar step-heating measurements. The step-heating release spectra are typically discordant, displaying a subtle to pronounced saddle shape, indicative of excess Ar. When the isotope results are cast upon an isotope correlation diagram, the results indicate that the DMV samples generally have initial ^{40}Ar/^{36}Ar ratios greater than that of atmospheric Ar (295), in-

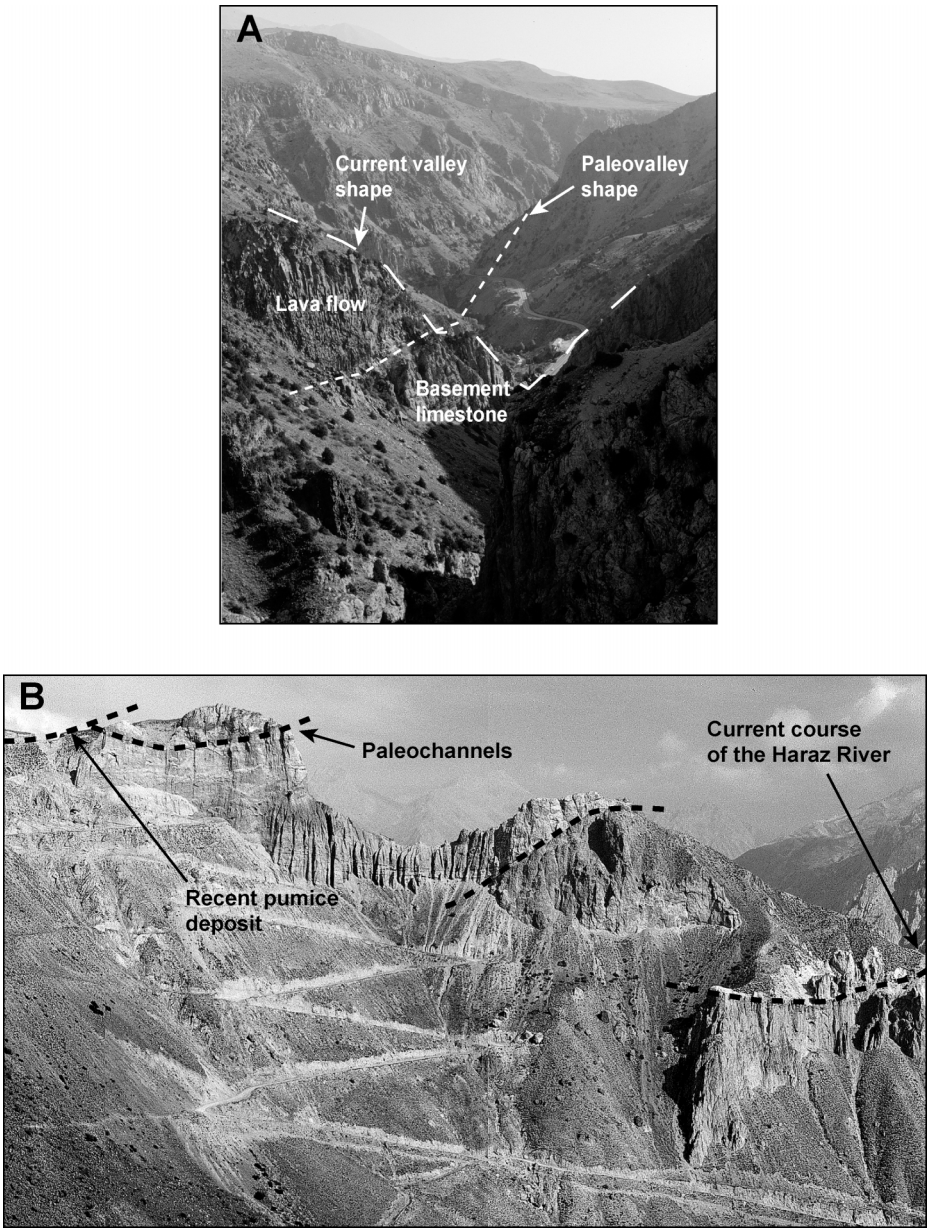

Figure 6. Examples of paleovalleys at Damavand volcano. (A) Paleovalley wall in Lar Limestone at the Ask Gorge. Main drainage has moved eastward (right) as a consequence of valley fill by the thick trachyandesite flow (DM12 dated at 25 ka). Valley is ~100 m across. (B) Paleovalleys in older volcaniclastic sequence at the head of Gazaneh Canyon. Haraz River runs perpendicular to exposures to the east. Width of image represents ~700 m.

dicating an excess ^{40}Ar component. Specifically, in all but two samples, the isochron data for the DMV samples indicate an initial $^{40}Ar/^{36}Ar$ ratio of ~300 or greater. Thus, in most cases, the isochron age is the preferred age estimate for the measured samples. The effect of the excess Ar component is most profound on the younger feldspar samples.

By means of an example, the step-heating spectrum for sample 97-DVM-17 is shown in Figure 8. The spectrum is discordant and has a distinct saddle shape. A plateau age of 65.6 ± 1.4 ka is defined, however, by six consecutive steps, from 675 to 950 °C, comprising ~70% of the total released ^{39}Ar. The integrated total-fusion age is 84 ± 2 ka, older than the plateau age by ca. 18 ka. These ages are discordant at the 95% confidence level. All the step-heating data except the highest-temperature step (1300 °C—dark diagonally ruled pattern in Fig. 8A) analytically define (at the 95% confidence level) a mixing line between an initial $^{40}Ar/^{36}Ar$ ratio of 301 ± 1.2 and an $^{40}Ar/^{39}Ar$ ratio corresponding to an age of 60.0 ± 1.7 ka and are used to determine the isochron age. Starting with the lowest-temperature step (600 °C), each increasing temperature step moves down and to the right along a mixing line until the 800 °C step. Subsequently, each increasing temperature step then moves back up and to the left, along the same mixing line until the 1200 °C step. The plateau age of 65.6 ± 1.4 ka is analytically indistinguishable from the isochron age (60.0 ± 1.7 ka) at the 95% confidence level. The $^{40}Ar/^{36}Ar_{init}$ ratio of 301 ± 1.2, however, is analytically distinguishable from atmospheric Ar; thus the isochron age is the analytically more correct age and is the preferred age estimate for this sample.

Note that the choice of most reliable Ar-Ar ages shown in Table 2 was independent of, and without knowledge of, the (U-Th)/He ages from apatites from the same samples, which are discussed below. In light of this fact, the general agreement between the two methods is good (Fig. 7B).

Apatite (U-Th)/He Dating

The ubiquitous presence of large apatite phenocrysts in Damavand trachyandesites has led us to attempt to date these apatite-bearing lavas by using (U-Th)/He geochronometry (e.g., Zeitler et al., 1987; Lippolt et al., 1994; Wolf et al., 1996; House et al., 1997; Farley, 2000; Stockli et al., 2000; Farley et al., 2000).

(U-Th)/He dating of apatite is based on the decay of ^{235}U, ^{238}U, and ^{232}Th by alpha (^{4}He nucleus) emission. Experimental observations on Durango apatite suggest a (U-Th)/He closure temperature of ~70 °C in apatite with a radius of ~80–90 μm. He diffusivity appears to correlate with the physical dimensions of the apatite crystal, indicating that the diffusion domain is the grain itself. Thus, grain size has a small effect on the closure temperature (Farley, 2000), as He diffusivity decreases with increasing grain size. Given the very large radius of analyzed Damavand apatite phenocrysts (~250–350 μm), the effective closure temperature (under the assumption of simple volume diffusion and a single domain size) is ~100 °C.

(U-Th)/He dating has been successfully employed to date tephras younger than 1 Ma (Farley et al., 2000). The Damavand dating is of particular interest as (1) apatites have been successfully dated with good precision and reproducibility (Table 3) down to ages as young as 7000 yr and (2) the (U-Th)/He apatite ages

TABLE 2. ISOTOPE DATES FOR DAMAVAND VOLCANIC ROCKS: DETAILS OF $^{40}Ar/^{39}Ar$ DATING

Sample	Description	Plateau age (ka)	Isochron age (ka)	MSWD	Total fusion age (ka)	$^{40}Ar/^{36}Ar$
DMV34 (feldspar)	Morphologically young flow, southwest flank	69 ± 11	**24 ± 7**†	1.9	230 ± 30	298.8 ± 9
DMV12 (feldspar)	Thick trachyandesite in Haraz Valley	51 ± 4	**24 ± 6**	4.7	230 ± 30	304.0 ± 2
DMV07 (biotite)	Flow by road, Poloor	117 ± 15	**14 ± 5**	1.0	106 ± 17	303.0 ± 1.6
DMV51 (feldspar)	Satellite vent south of summit	No plateau	5 ± 1	3.4	–	308.6 ± 1.8
DMV51 (biotite)	Satellite vent south of summit	63 ± 15	**26 ± 8**	1.5	84 ± 16	302 ± 5
DMV17 (feldspar)	Flow from roadcut in upper Poloor-Renne road	65.6 ± 1	**60.0 ± 2**	4.0	84 ± 2	301.8 ± 1.7
DMV19G (biotite)	Gray pumice from working quarry south of Renne	201 ± 6	**156 ± 7**	1.0	263 ± 13	300.4 ± 0.7
DMV116 (feldspar)	Upper flow in canyon at Hajidella	**170 ± 3**	167 ± 7	1.9	197 ± 5	295.6 ± 1.9
DMV13 (feldspar)‡	Ask Ignimbrite, just north of Ask	269 ± 12	230 ± 2	0.9	278 ± 14	304 ± 9
DMV13 (biotite)	Ask Ignimbrite, just north of Ask	293 ± 14	270 ± 8	0.3	298 ± 14	298 ± 11
DMV114 (feldspar	Bottom flow, Sardobitch, above Nandal	**1034 ± 8**	1008 ± 10	5.6	1069 ± 9	324 ± 4
DMV108 (feldspar)	Top flow, Sardobitch, above Nandal	**967 ± 8**	968 ± 8	1.7	–	295.5

†Ages in bold represent preferred Ar ages—see text for explanation. Errors given are 1σ for consistency with other Ar dating studies and for ease of use in statistical tests.

‡Preferred age = **281 ± 8**; combined feldspar-biotite isochron.

Table 3. ISOTOPE DATES FOR DAMAVAND VOLCANIC ROCKS: DETAILS OF APATITE (U-Th)/He DATING

Sample	Description	Age (ka)	2σ (ka)	s.d.† (ka)	U (ppm)	Th (ppm)	He (nmol/g)	Mass (mg)	F_t	r (μm)	*n*
Young Damavand											
DMV126S	Morphologically young flow, southwest flank	7.3	0.2	0.3	7.3	49.4	0.001	2298.1	0.96	306.4	3
DMV34	Morphologically young flow, southwest flank	7.3	0.2	0.1	9.9	70.8	0.001	1113.8	0.95	225.0	3
DMV12	Thick trachyandesite in Haraz Valley	25.4	0.8	0.6	10.6	76.3	0.004	1383.6	0.95	258.8	3
DMV07	Flow by road, Poloor	27.1	0.8	0.2	5.8	40.4	0.002	2594.4	0.97	388.5	2
DMV17	Flow from roadcut in upper Poloor-Renne road	66.5	2.0	12.0	6.5	41.9	0.006	727.1	0.94	198.6	4
DMV305	Breccia fragment from Vanha debris avalanche	168.3	5.0	14.2	0.1	0.4	0.000	709.3	0.94	202.8	2
DMV39	Thin pumice and ash flow, southwest flank	177.2	5.3	2.2	10.6	78.2	0.026	884.4	0.94	196.4	2
DMV19G	Gray pumice from working quarry south of Renne	177.9	5.3	0.2	10.4	81.3	0.027	885.3	0.94	198.6	2
DMV116	Upper flow in canyon at Hadjidella	194.8	5.8	1.6	9.9	76.0	0.028	2181.4	0.97	348.6	2
DMV335	Pumice below debris avalanche, near Hadjidella	224.8	6.7	3.6	11.0	81.3	0.035	1124.5	0.94	224.3	2
DMV312	Ignimbrite from east of Hadjidella	264.2	7.9	6.1	10.3	76.1	0.039	1312.5	0.95	240.7	2
DMV13	Ask Ignimbrite, just north of Ask	279.9	8.4	5.8	11.0	81.6	0.043	753.4	0.94	220.0	2
DMV147	Lowermost flow in valley-wall section south of Ask	445.8	13.4	6.2	7.1	48.0	0.042	1599.9	0.95	240.0	2
Old Damavand											
DMV309	Clast from breccia in hydrothermally altered vent area, Gazaneh Canyon	544.5‡	16.3	3.0	7.9	56.7	0.059	813.9	0.94	200.4	2
DMV132a	Trachyandesite clast in sediments Poloor formation	812.5	24.4	2.7	7.1	50.3	0.081	1856.6	0.96	369.0	2
DMV04	Flow on east side of valley, Poloor	813.5	24.4	1.7	6.0	48.8	0.073	905.5	0.95	235.2	2
DMV114	Bottom flow, Sardobitch, above Nandal	1046.9	52.3	12.6	7.6	56.9	0.114	901.9	0.95	264.3	2
DMV108	Top flow, Sardobitch, above Nandal	1197.1	59.9	8.9	8.7	68.3	0.154	916.0	0.96	316.5	2
DMV131	Pumice clasts in sediments of Poloor formation	1776.2	53.3	43.6	4.1	32.5	0.103	325.4	0.90	122.6	2

†s.d.—calculated standard deviation of individual analyses (measure of reproducibility); Ft—alpha ejection correction after Farley et al. (1996); r—apatite crystal radius; n—number of analyses.

‡Sample is stratigraphically part of Old Damavand. Age probably represents resetting of (U-Th)-He systematics by Young Damavand activity.

can be checked against $^{40}Ar/^{39}Ar$ ages on many of the same samples, with generally good agreement.

Apatite (U-Th)/He ages are given in Table 3, and sample locations in Figure 1. Samples were collected away from the tops of individual lava flows to avoid thermal resetting of the apatite (U-Th)/He clocks during the subsequent emplacement of younger trachyandesite flows. All reported ages are weighted mean averages of two to four individual analyses that are reproducible to better than 1%. Ages are calculated by assuming secular equilibrium. Error in this assumption might affect ages derived from the youngest Damavand flows, but should not affect samples older than 100 ka, which is corroborated by the agreement of (U-Th)/He and $^{40}Ar/^{39}Ar$ analyses (Fig. 7B).

DISCUSSION AND INTERPRETATION

Volcanism began at least 1.8 m.y. ago at Damavand volcano, although evidence for significant activity is not preserved until ca. 1.2 Ma. The data suggest three periods of significant eruptive activity—ca. 1.2 Ma to 800 ka, ca. 280 ka to 150 ka, and ca. 60 ka to 7 ka (Fig. 7A)—although whether these ages are distinct periods of major activity, or simply the result of preservational/sampling bias, remains unclear. Major rearrangements of magma systems in stratovolcanoes are typically accompanied by distinct changes in the compositions of the erupted products (e.g., Singer et al., 1997). At Damavand volcano, the compositions of materials erupted are remarkably homogeneous over >1 m.y. (Fig. 3). Furthermore, the lack of very abrupt changes in the character of the volcaniclastic sediments in the Haraz drainage, even at horizons marking significant events in the history of the volcano such as the ignimbrite eruption and the sector collapse, suggests that there may have been no protracted (>500 k.y.) period of dormancy/extinction. The distinction between the Old and Young cones is therefore based largely on the unconformable relationships in Gazaneh Canyon (Fig. 2A) and the presence of distinctly hydrothermally altered vent area rocks of Old Damavand overlain by fresh lavas of Young Damavand. Altered clasts are common in the lowest parts of the volcaniclastic succession, most notably in the northeastern (Hadjidella) sector. The influence that the sector-collapse event may have had on the erosion of the volcano and on the shift from Old to Young Damavand is unknown.

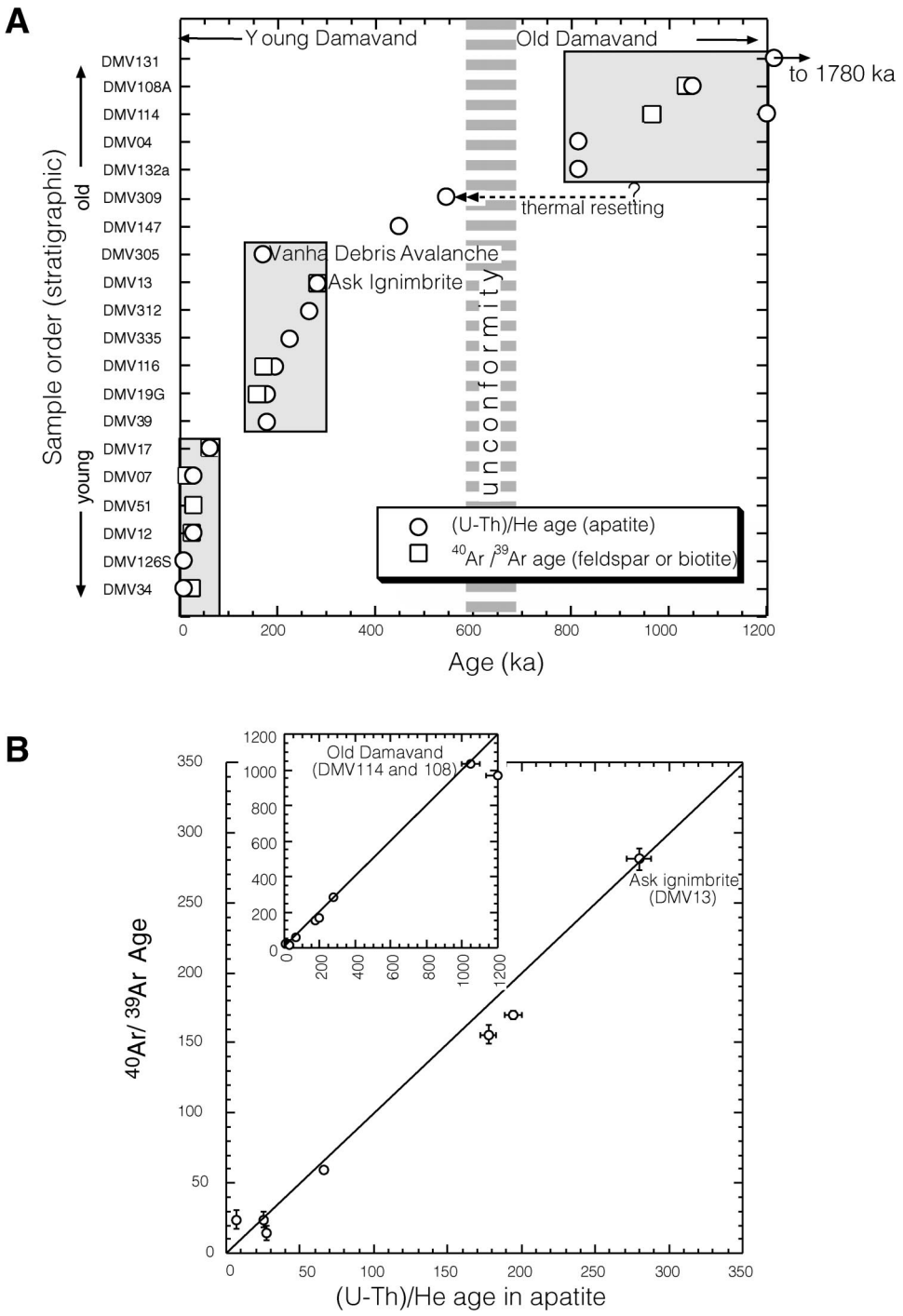

Figure 7. (A) Isotope dates for Damavand rocks, showing the tendency for discrete episodes of cone building (gray boxes) and the temporal distinction between the Old and Young cones (vertical dashed line)—thought to correspond to a period of dormancy and erosion accompanied by a shift in vent location. Stratigraphic order is based on field relationships to the best extent possible—the Ask Ignimbrite (DMV13) clearly overlies the Vahna debris avalanche, the apatite (U-Th)/He age of which is assumed therefore to be in error. Also, DMV108 clearly overlies DMV114 in a succession up Sardobitch Ridge. Here the Ar ages are consistent with stratigraphy, whereas apatite (U-Th)/He ages are not. (B) Comparison between $^{40}Ar/^{39}Ar$ ages and (U-Th)/He in apatite ages, showing fairly close agreement (most samples plot close to 1:1 line). Inset has expanded age scale to show two Old Damavand samples. Where ages are not in agreement, the tendency is for (U-Th)/He dates to be slightly older.

Activity from ca. 1.8 Ma to 800 ka: Old Damavand

The oldest eruption age (ca. 1.78 Ma) is given by DMV131, a reworked trachyandesite pumice toward the base of the Poloor formation. Old Damavand eruptions at ca. 810 ka (DMV04 and DMV132a) produced trachyandesite flows, evidence for which is now found as clasts in the upper part of the Poloor formation. This underscores our interpretation that the Poloor formation is older than the other volcaniclastic rocks and is a partial record of the history of Old Damavand from ca. 1.78 m.y. to ca. 812 k.y. These ages also indicate that the olivine basalts intercalated in the lower part of the Poloor formation predate ca. 812 ka. Two other Old Damavand lavas from the northern ridge (Sardobitch; DMV108 and DMV114) yield (U-Th)/He ages of 1197 ± 60 ka and 1047 ± 52 ka, respectively, although these ages are not consistent with stratigraphic relationships because the DMV108 flow overlies the flow yielding sample DMV114. The $^{40}Ar/^{39}Ar$ dates are consistent with stratigraphic order and are in agreement for DMV114. Given that the $^{40}Ar/^{39}Ar$ age of DMV108 is the best behaved of all the analyzed samples, it would appear that the apatite age of DMV108 is too old.

Activity from ca. 600 ka to 150 ka

Activity at Young Damavand probably began at ca. 500–600 ka. The flow that yielded sample DMV147, dated as 445 ka, underlies the Ask formation to the south of Ask and is succeeded by a thick succession of trachyandesites that are capped by a flow at 60 ka (DMV17). The breccia yielding sample DMV309 (550 ka) is stratigraphically part of Old Damavand, and we suggest that the (U-Th)/He age has been thermally reset by its proximity to the vent region of Young Damavand. This interpretation means that the oldest record of activity from the young cone dates to ca. 550 ka and that the unconformity between the two edifices occupies the gap in activity between this age and ca. 800 ka.

The Ask Ignimbrite (DMV13; 280 ka) does provide a useful reference marker horizon in sections along the Haraz River valley, where it can be confidently traced for some 20 km northward from Ask Gorge. The Vahna debris avalanche is also found in several places along the Haraz River, where it clearly underlies the Ask Ignimbrite, despite younger (U-Th)/He ages, which must accordingly be in error (Fig. 7A). Ignimbrite and debris avalanche deposits are found in the Hadjidella region, although the relationship between them is more ambig-

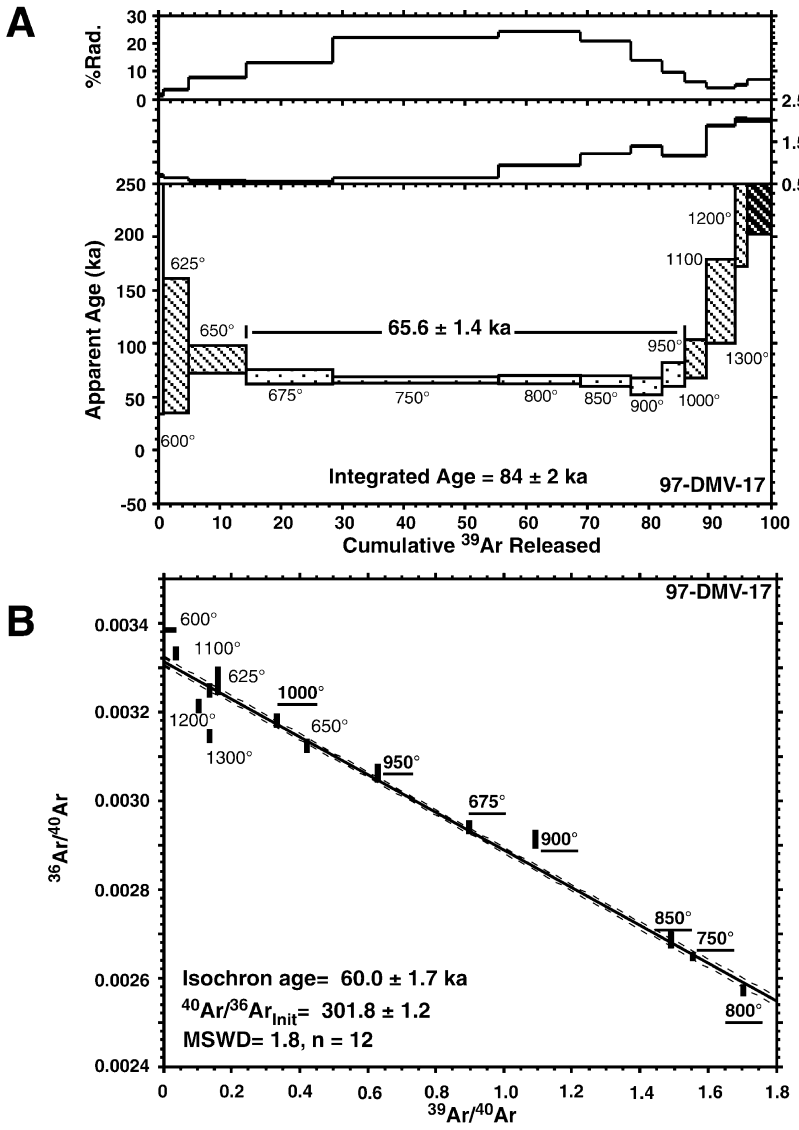

Figure 8. (A) Step-heating spectrum and plateau diagram for sample 97-DMV-17. The pattern and behavior indicated in these figures are typical of the DMV samples. The plateau, indicated by a widely spaced dot pattern, is defined by six consecutive steps from 675 to 950 °C and is composed of ~70% of the total released ^{39}Ar. (B) In the isochron plot, the symbols represent the 1σ error ellipses, and the bold underlined labels correspond to the plateau steps. The isochron plot for these data indicates a well-defined mixing line between an initial ^{40}Ar/^{36}Ar ratio of 301 ± 1.2 and an ^{40}Ar/^{39}Ar ratio corresponding to an age of 60.0 ± 1.7 ka. The samples were analyzed by using a double-vacuum resistance furnace at Lamont-Doherty. Typical procedural banks for this system (both the room temperature and at 1000 °C blank, respectively) are as follows: ^{40}Ar 0.8–1.0 × 10^{-11} cm^3, ^{39}Ar 0.9–1.5 × 10^{-14} cm^3, ^{38}Ar: 6.0–6.5 × 10^{-15} cm^3, ^{37}Ar: 1.2–7.2 × 10^{-16} cm^3, ^{36}Ar: 3.0–3.6 × 10^{-14} cm^3 (all volumes at STP [standard temperature and pressure]). Gas yields for samples are typically 50 or more times larger than the procedural blanks.

uous as the outcrops are separated. To the east of Hadjidella, in sections topographically high above the Haraz River, we have found restricted erosional remnants of an unwelded ignimbrite that appears to be the same as the Ask Ignimbrite, or at least temporally related (DMV312; 264.2 ± 17.9 ka, Table 3). A debris avalanche is found toward the top of the section at Hadjidella; the possibilities are that there may be two (or more) sector-collapse events of different ages or that the ignimbrite near Hadjidella is not equivalent to the Ask Ignimbrite. Dating of a pumice unit that occurs below the debris avalanche deposit at Hadjidella (DMV335; 224.8 ± 6.7 ka, Table 3) suggests that it is not the stratigraphic equivalent of the Vahna debris avalanche, but rather a distinct, younger deposit. The Hadjidella section is capped by trachyandesite flow DMV116 (Fig. 2B) dated at ca. 170 ka by ^{40}Ar/^{39}Ar (25 k.y. older by (U-Th)/He). The Hadjidella formation (including the debris avalanche) must therefore be older than 170 k.y. An age of ca. 170–180 ka also corresponds to the widely distributed pumice deposits on the upper flanks of the volcano (DMV19G). These appear to be age-correlative with the small pyroclastic flows of the southwest flank (DMV39).

Activity from ca. 60 ka to 7 ka

A protracted period of eruptions on the southern flank is bracketed by DMV17 (ca. 60 ka) and the (ca. 25 ka) thick flows (DMV07 and DMV12) that appear to have filled in the Haraz River valley in places. An ^{40}Ar/^{39}Ar age of 26 ka was also obtained for DMV51, the satellite center on the south flank. Although preserving some youthful morphological characteristics such as flow levees, all of the south flank lavas are clearly (by virtue of more extensive degradation and vegetation cover) older than the Holocene flows of the western flanks. A ca. 7.3 ka eruption (DMV34 and DMV126S) on the western side of Damavand volcano forms the morphologically youngest flows that still preserve flow-top breccias and distinct flow levees. The Ar age (plateau or isochron) for DMV34 is considerably older (older than 20 ka) and difficult to reconcile with the morphology and lack of glaciation.

History of the Damavand Region (Fig. 9)

The earliest eruptions of Damavand volcano began at ca. 1.8 Ma. This may not have been an extensive eruptive period, or there may have been a long period of dormancy that allowed erosion of erupted material to occur. In the Poloor region, olivine basalt flows were erupted from local cinder cones. The precise age of these olivine basalt flows is unknown, although they infill canyons cut into the Poloor formation sediments, which, in turn, were deposited over the period of at least 1776–812 ka (Table 3). The valley-filling distribution of the basalts indicates that a drainage system ancestral to the current Haraz River existed at the time.

At ca. 1.1–0.8 Ma, a large trachyandesite volcano, broadly similar to the modern cone, existed (Fig. 9A). The vent region lay just to

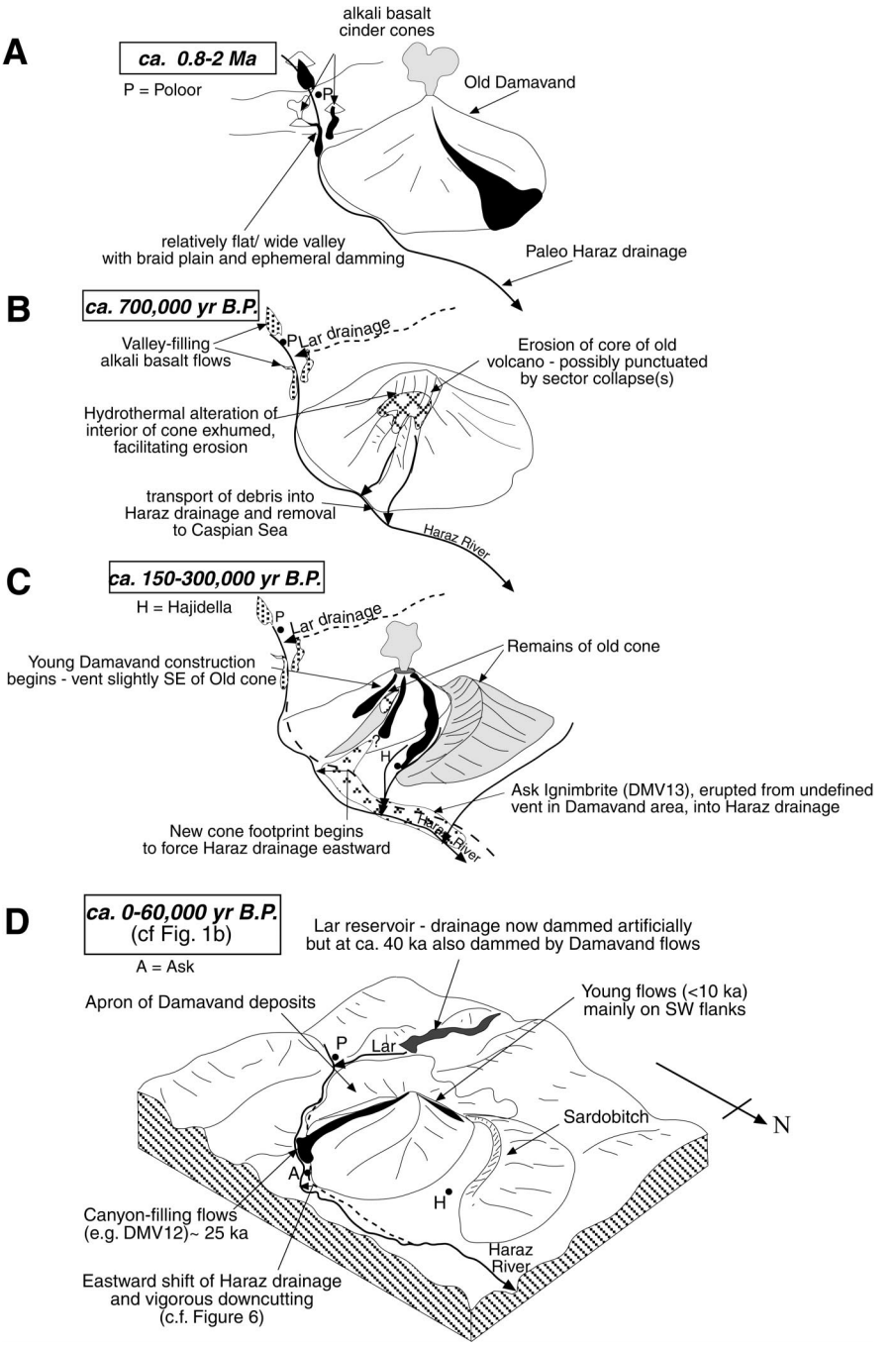

Figure 9. Evolution of Damavand volcanic edifice illustrated in a series of cartoons. See text for explanation.

the northeast of the present summit and is currently exposed in the head of Gazaneh Canyon. The northern flank of this volcano is preserved as the arcuate ridge of Sardobitch, but clasts thought to be related to Old Damavand are present as far southeast as Poloor.

A period of extensive erosion exhumed Old Damavand and transported volcaniclastic debris into the Haraz drainage and beyond to the Caspian Sea (Fig. 9B). Remnant deposits are exposed in the Haraz drainage and in the broad eroded swale between Sardobitch and the current cone (Hadjidella region). The last Old Damavand eruptions probably occurred at ca. 800 ka, allowing for ~300,000 yr of erosion.

Young Damavand has been active since at least 500 ka. ''Older flows'' from this period (DMV147 at ca. 446 ka) are overlain by the Ask formation and cap the Hadjidella formation (DMV 116 at ca. 195 ka). The Ask Ignimbrite was erupted into the Haraz drainage at ca. 250 ka. A relatively large-scale pyroclastic eruption (represented by DMV19G) occurred at ca. 178 ka, and the corresponding (commonly reworked) fallout deposits overlie many of the older lava flows (Fig. 9C).

Younger flows (younger than 100 ka) are clearly associated with the morphology of the present cone. The radially disposed young flows are concentrated on the steep western flanks, perhaps obstructed to the east by the vestiges of the old cone that still presented a topographic barrier. The only significant satellite vent found erupted during this period (26 ka). The most recent eruptive episode dated occurred at 7300 yr B.P., forming small, morphologically young (unglaciated and unvegetated) flows on the western flanks of the current cone (Fig. 9D).

It is possible that the Haraz River drainage became more accentuated only recently. The extensive down-valley traces of individual fluvial or lahar deposits are more consistent with deposition on a broad flat-bottomed valley rather than in a steep-sided gorge such as seen today. Furthermore, the fluvial deposits in the Ask formation, which overlie the Ask Ignimbrite and are therefore younger than 250 ka, requires downcutting at a minimum rate of ~1 km/m.y. Remnant terraces 200–500 m above the current valley floor may also signify recent rejuvenation.

CONCLUSIONS

1. The cone comprises >400 km^3 of rather uniform porphyritic trachyandesites, which share broadly intraplate trace element characteristics with small-volume alkali olivine basalts found in the region. Magmatism may be due to decompression melting in response to lithospheric delamination beneath the Alborz Mountains.

2. $^{40}Ar/^{39}Ar$ (feldspar or biotite) and (U-Th)/He (apatite) dates agree well with each other and define an overall protracted range of volcanic activity from 1.8 Ma to 7 ka. The current cone (Young Damavand; ca. 600–7 ka) lies slightly south of the eroded remnants of the Old Damavand cone (ca. 1780–800 ka).

3. Volcanic activity consisted principally of relatively small volume individual effusive eruptions from strongly localized (summit) vents; these eruptions were punctuated by occasional pyroclastic eruptions that generated fall or flow deposits compositionally identical to the lavas. Valley-filling remnants of an originally extensive ignimbrite (the Ask Ignimbrite; 280 ka) and a debris avalanche (the Vahna debris avalanche; lying below the Ask

Ignimbrite) are the only significant lithologic markers of major events at the volcano.

4. Preserved volcaniclastic deposits provide a more complete record of volcano history than the volcanic rocks of the current edifice. Nevertheless, even the extensive volcaniclastic successions encountered in major drainages are incomplete as a result of rapid erosion and reworking. A more complete record of volcanogenic material may be preserved in the ultimate sink of local sedimentary systems, the Caspian Sea Basin.

ACKNOWLEDGMENTS

This research was supported by the National Research Council of the Islamic Republic of Iran (NRCI) as a National Research Project under grant number 31303335 and by the U.S. National Science Foundation under grant number EAR-9627923. Amy Young is thanked for her efforts in the field and laboratory in the early stages of this work. We thank the Institute of Geophysics, Tehran University, for logistical assistance and the Iranian Remote Sensing Center for data for Figure 1B. (U-Th)/He work was conducted at Caltech and was supported by a Caltech postdoctoral fellowship (to Stockli) and a Packard Foundation fellowship (to K.A. Farley). Dougal Jerram and Gary Axen contributed valuable assistance in the field, and Teresa Lassak assisted with mineral separations. Early versions of the manuscript were improved following review by Dougal Jerram. Anita Grunder and an anonymous reviewer, along with editors Scott Baldridge, Allen Glazner, and Yildirim Dilek, provided suggestions and comments that greatly improved the manuscript.

REFERENCES CITED

Allenbach, P., 1966, Geologie und petrographie des Damavand und seiner umgeurg (Zentral-Elburz): Iran: Geologisches Institut, ETH-Zurich, Mitteilung Nr. 63, 114 p.

Axen, G.J., Lam, P.S., Grove, M., Stockli, D.F., and Hassanzadeh, J., 2001, Exhumation of the west-central Alborz Mountains, Iran, Caspian subsidence, and collision-related tectonics: Geology, v. 29, p. 559–562.

Berberian, M., 1983, The southern Caspian: A compressional depression floored by a trapped, modified oceanic crust: Canadian Journal of Earth Sciences, v. 20, p. 163–183.

Berzins, R., 2001, The stratigraphic and volcano-sedimentary record of Damavand volcano, northern Iran [M.S. thesis]: Los Angeles, University of California, 204 p.

Brousse, R., Lefevre, C., Maury, R.C., Moine-Vaziri, H., and Aminie-Sobhani, E., 1977, Le Damavand: Un volcan shoshonitique de la plaque iranienne: Paris, Comptes Rendus de l'Académie des Sciences, Serie D, v. 285, p. 131–134.

Cartier, E., 1972, Geological map of the central Alborz: Sheet Damavand: Tehran, Iran, Geological Survey, scale 1:100,000, 1 sheet.

Davidson, J.P., and Wilson, I.R., 1989, Evolution of an alkali basalt–trachyte suite from Jebel Marra volcano, Sudan, through assimilation and fractional crystallization: Earth and Planetary Science Letters, v. 95, p. 141–160.

Davidson, J.P., McMillan, N.J., Moorbath, S., Worner, G., Harmon, R.S., and Lopez-Escobar, L., 1990, The Nevados de Payachata volcanic region (18°S, 69°W, N. Chile): II. Evidence for widespread crustal involvement in Andean magmatism: Contributions to Mineralogy and Petrology, v. 105, p. 412–432.

Davidson, J.P., Hassanzadeh, J., Berzins, R., Pandamouz, A., Turrin, B., and Young, A., 2000, Magmagenesis and evolution at Damavand volcano, Iran: Journal of Conference Abstracts, v. 5, p. 334.

Dehghani, G.A., and Makris, J., 1984, The gravity field and crustal structure of Iran: Neues Jahrbuch für Geologie und Palaontologie Abhandlungen, v. 168, p. 215–229.

Dewey, J.F., and Şengör, A.M.C., 1979, Aegean and surrounding regions: Complex multiple and continuum tectonics in a convergent zone: Geological Society of America Bulletin, v. 90, p. 84–92.

Dilek, Y., and Moores, E.M., 1999, A Tibetan model for the early Tertiary western United States: Geological Society [London] Journal, v. 156, p. 929–942.

Farley, K.A., 2000, Helium diffusion from apatite: General behavior as illustrated by Durango fluorapatite: Journal of Geophysical Research, v. 105, p. 2903–2914.

Farley, K.A., Kohn, B.P., and Stockli, D.F., 2000, (U-Th)/He dating of Quaternary tephras and lavas: Geological Society of America Abstracts with Programs, v. 32, no. 7, p. 325.

Farley, K.A., Wolf, R.A., and Silver, L.T., 1996, The effects of long alpha-stopping distances on (U-Th)/He dates: Geochemica et Cosmochimica Acta, v. 60, p. 4223–4229.

Ferrigno, J.G., 1991, Glaciers of the Middle East and Africa—Glaciers of Iran, *in* Williams, R.S., and Ferrigno, J.G., eds., Glaciers of the Middle East and Africa: U.S. Geological Survey Professional Paper 1386-G, p. G31–G47.

Hassanzadeh, J., 1994, Consequence of the Zagros continental collision on the evolution of the central Iranian plateau: Journal of Earth and Space Physics, v. 21, p. 27–38.

House, M.A., Wernicke, B.P., Farley, K.A., and Dumitru, T.A., 1997, Cenozoic thermal evolution of the central Sierra Nevada, California, from (U-Th)/He thermochronometry: Earth and Planetary Science Letters, v. 151, p. 167–179.

Jung, D., Kursten, M., and Tarakian, M., 1976, Post-Mesozoic volcanism in Iran and its relation to the subduction of the Afro-Arabian under the Eurasian plate, *in* Pilger, A., and Rosler, A., eds., Afar between continental and oceanic rifting (Volume II): Stuttgart, Schweizerbatsche Verlagsbuch-handlung, p. 175–181.

Kadinsky-Cade, K., Barazangi, M., Oliver, J., and Isacks, B., 1981, Lateral variations of the high-frequency seismic wave propagation at regional distances across the Turkish and Iranian plateaus: Journal of Geophysical Research, v. 86, p. 9377–9396.

Lippolt, H.J., Leitz, M., Wernicke, R.S., and Hagedorn, B., 1994, (Uranium+thorium)/helium dating of apatite: Experience with samples from different geochemical environments: Chemical Geology, v. 112, p. 179–191.

Mehdizadeh, H., Liotard, J.-M., and Dautria, J.-M., 2002, Geochemical characteristics of an intracontinental shoshonitic association: The example of the Damavand volcano, Iran: Comptes Rendus Geosciences, v. 334, p. 111–117.

Pandamouz, A., 1998, A new investigation of stratigraphic position of the basaltic flows in the volcanic sequence of Damavand (central Alborz, northern Iran) [M.S. thesis]: Tehran, Iran, Tehran University, 153 p.

Pearce, J.A., 1982, Trace element characteristics of lavas from destructive plate boundaries, *in* Thorpe, R.S., ed., Andesites: Chichester, New York, John Wiley and Sons, p. 525–547.

Pearce, J.A., and Norry, M.J., 1979, Petrogenetic implications of Ti, Zr, Y and Nb variations in volcanic rocks: Contributions to Mineralogy and Petrology, v. 69, p. 33–47.

Pearce, J.A., Bender, J.F., De Long, S.E., Kidd, W.S.F., Low, P.J., Guner, Y., Saroglu, F., Yilmaz, Y., Moorbath, S., and Mitchell, J.G., 1990, Genesis of collisional volcanism in eastern Anatolia, Turkey: Journal of Volcanology and Hydrothermal Research, v. 44, p. 189–229.

Priestley, K., Baker, C., and Jackson, J., 1994, Implications of earthquake focal mechanism data for the active tectonics of the south Caspian basin and surrounding regions: Geophysical Journal International, v. 118, p. 111–141.

Schmincke, H.U., 1974, Volcanological aspects of peralkaline silicic welded ash flow tuffs: Bulletin of Volcanology, v. 38, p. 594–636.

Singer, B.S., Thompson, R.A., Dungan, M.A., Feeley, T.C., Nelson, S.T., Pickens, J.C., Brown, L.L., Wulff, A.W., Davidson, J.P., and Metzger, J., 1997, Volcanism and erosion during the past 930 k.y. at the Tatara–San Pedro Complex, Chilean Andes: Geological Society of America Bulletin, v. 109, p. 127–142.

Stockli, D., Farley, K., and Dumitru, T., 2000, Calibration of the apatite (U-Th)/He thermochronometer on an exhumed fault block, White Mountains, California: Geology, v. 28, p. 983–986.

Stocklin, J., 1974, Northern Iran: Alborz Mountains, *in* A.M., Spencer, ed., Mesozoic–Cenozoic orogenic belts data for orogenic studies; Alpin—Himalayan Orogens: Geological Society [London] Special Publication 4, p. 212–234.

Stocklin, J., 1977, Structural correlation of the Alpine ranges between Iran and central Asia: Société Géologique de France, Memoire hors série, v. 8, p. 333–353.

Sun, S.-S., and McDonough, W.F., 1989, Chemical and isotopic systematics of oceanic basalts: Implications for mantle compositions and processes, *in* Saunders, A.D., and Norry, M.J., eds., Magmatism in the ocean basins: Geological Society [London] Special Publication 42, p. 313–345.

Toksoz, M.N., and Bird, P., 1977, Formation and evolution of marginal basins and continental plateaus, *in* Talwani, M., and Pitman, W.C., III, eds., Island arcs, deep sea trenches and backarc basins: American Geophysical Union Maurice Ewing Series 1, p. 379–393.

Turrin, B.D., Christiansen, R.L., Clynne, M.A., Champion, D.E., Gerstel, W.J., Muffler, L.J.P., and Trimble, D.A., 1998, Age of Lassen Peak, California, and implications for the ages of late Pleistocene glaciations in the southern Cascade Range: Geological Society of America Bulletin, v. 110, p. 931–945.

Wolf, R.A., Farley, K.A., and Silver, L.T., 1996, Helium diffusion and low-temperature thermochronometry of apatite: Geochimica et Cosmochimica Acta, v. 60, p. 4231–4240.

Wolff, J.A., and Wright, J.V., 1981, Rheomorphism of welded tuffs: Journal of Volcanology and Geothermal Research, v. 10, p. 13–34.

Wood, D.A., 1980, The application of a Th-Hf-Ta diagram to problems of tectonomagmatic classification and to establishing the nature of crustal contamination of basaltic lavas of the British Tertiary volcanic province: Earth and Planetary Science Letters, v. 50, p. 11–30.

Wörner, G., Harmon, R.S., Davidson, J.P., Moorbath, S., Turner, D.L., McMillan, N.J., Nye, C., Lopez-Escobar, L., and Moreno, H., 1988, The Nevados de Payachata volcanic region (18°S/69°W, N. Chile): I. Geological, geochemical and isotopic observations: Bulletin of Volcanology, v. 50, p. 287–303.

Young, A.E., Davidson, J.P., and Hassanzadeh, J., 1998, Preliminary constraints on magma genesis at Damavand volcano, Iran: Capetown, South Africa, IAVCEI Congress Abstracts, p. 72.

Zeitler, P.K., Herczig, A.L., McDougall, I., and Honda, M., 1987, U-Th-He dating of apatite: A potential thermochronometer: Geochimica et Cosmochimica Acta, v. 51, p. 2865–2868.

MANUSCRIPT RECEIVED BY THE SOCIETY 24 FEBRUARY 2003
REVISED MANUSCRIPT RECEIVED 27 JUNE 2003
MANUSCRIPT ACCEPTED 12 JULY 2003

Printed in the USA